MICROCOPY RESOLUTION TEST CHART

NATIONAL BUREAU OF STANDARDS-1963-A

AD-E300542

42

LEVEL III

DNA 4715Z

SHOCK EFFECTS IN CARBONATES

Joana Vizgirda
Thomas J. Ahrens

California Institute of Technology
Seismological Laboratory
Division of Geological and
   Planetary Sciences
Pasadena, California 91125
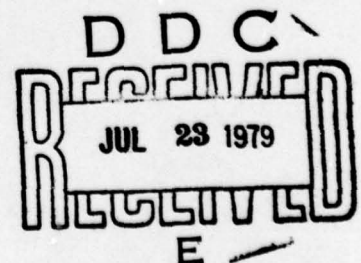
28 February 1977

Interim Report for Period 1 March 1976 — 28 February 1977

CONTRACT No. DNA 001-76-C-0218

DDC
RECEIVED
JUL 23 1979
E

DDC FILE COPY

Prepared for
Director
DEFENSE NUCLEAR AGENCY
Washington, D. C. 20305

79 06 06 001

Destroy this report when it is no longer
needed. Do not return to sender.

PLEASE NOTIFY THE DEFENSE NUCLEAR AGENCY,
ATTN: TISI, WASHINGTON, D.C. 20305, IF
YOUR ADDRESS IS INCORRECT, IF YOU WISH TO
BE DELETED FROM THE DISTRIBUTION LIST, OR
IF THE ADDRESSEE IS NO LONGER EMPLOYED BY
YOUR ORGANIZATION.

REPORT DOCUMENTATION PAGE		READ INSTRUCTIONS BEFORE COMPLETING FORM
1. REPORT NUMBER DNA 4715Z	2. GOVT ACCESSION NO.	3. RECIPIENT'S CATALOG NUMBER
4. TITLE (and Subtitle) SHOCK EFFECTS IN CARBONATES		5. TYPE OF REPORT & PERIOD COVERED Interim Report for Period 1 Mar 76— 28 Feb 77
		6. PERFORMING ORG. REPORT NUMBER CIT-SL-SWL-1
7. AUTHOR(s) Joana Vizgirda and Thomas J. Ahrens		8. CONTRACT OR GRANT NUMBER(s) DNA 001-76-C-0218
9. PERFORMING ORGANIZATION NAME AND ADDRESS California Institute of Technology, Seismological Laboratory, Division of Geological and Planetary Sciences, Pasadena, California 91125		10. PROGRAM ELEMENT, PROJECT, TASK AREA & WORK UNIT NUMBERS Subtask Y99QAXSA001-89
11. CONTROLLING OFFICE NAME AND ADDRESS Director Defense Nuclear Agency Washington, D.C. 20305		12. REPORT DATE 28 February 1977
		13. NUMBER OF PAGES 22
14. MONITORING AGENCY NAME & ADDRESS(if different from Controlling Office)		15. SECURITY CLASS (of this report) UNCLASSIFIED
		15a. DECLASSIFICATION/DOWNGRADING SCHEDULE

16. DISTRIBUTION STATEMENT (of this Report)

Approved for public release; distribution unlimited.

17. DISTRIBUTION STATEMENT (of the abstract entered in Block 20, if different from Report)

19. KEY WORDS (Continue on reverse side if necessary and identify by block number)

Eniwetok Peak Pressures
Pacific Test Site
Shock Waves
Cratering

20. ABSTRACT (Continue on reverse side if necessary and identify by block number)
Permanent deformation of very small crystallites of carbonate minerals, such as those occurring in the Eniwetok core, has been examined using the following techniques: (a) Peak broadening of X-ray powder diffractometer patterns due to decreasing effective grain size with increasing shock deformation is observed. This effect is clearly seen in the core material taken from directly under the Cactus explosion. (b) Angular strain in calcite single crystals has been observed in Debye-Scherrer patterns of laboratory shocked samples and single-

D (over)

DD FORM 1473 EDITION OF 1 NOV 65 IS OBSOLETE

20. ABSTRACT (Continued)

(approximately)

crystallites from the Eniwetok core. Tentative peak shock pressures of ~8 kbar at a depth of ~15 m decaying to ~3 kbar at a depth of ~30 m are inferred on the basis of very preliminary data. (c) Shock-induced erasure of defect spectra, as examined by electron-spin resonance (ESR) techniques, is observed in carbonate material, both shocked in the laboratory and by the Cactus explosion. This effect is yet "uncalibrated." (d) Also using the ESR techniques, a systematic loss of fine structure of the resonance of Mn^{++} impurities in calcite is observed with increasing shock pressure, both in laboratory shocked samples and those in the Cactus core.

$Mn(++)$

PREFACE

We appreciate the encouragement and help of Jerry Stockton (RDA), David Roddy (USGS), and F. Tsay (JPL) have given us in this work. The introduction to the problem area presented to us by Captains B. Ristvet and W. Ullrich of AFWL, and the superb X-ray diffraction work carried out under Captain Robert Couch, McClellan AFB were important to achieving many of the results summarized in this report.

TABLE OF CONTENTS

INTRODUCTION

During the previous year, we have both developed quantitative criteria for
determining the peak shock stresses experienced by carbonate rocks, and applied
these to infer the peak shock pressure history of carbonate core (XC-1) mate-
rials recovered from ground zero beneath the Cactus explosion crater at Eniwetok.
Our efforts were directed toward three simultaneously conducted research phases:
a) the development of quantitative methods of shock effect analyses, b) careful
application of these methods to Cactus core material, and c) comparison of Cactus
core results with analagous carbonate rocks experimentally shocked in the labora-
tory to known stress levels.

The first of these phases demanded the greatest expenditure of effort, and
the techniques that have been developed are still in a process of refinement.
Due to the nature of the core material, an inhomogeneous, very fine-grained
biogenic carbonate, traditional optical methods of shock effect documentation
have, to date, proved to be unproductive. Application of X-ray and electron
spin resonance techniques was subsequently attempted; the resulting data appear
to be quantitatively relatable to the stress levels imposed on carbonate rocks.
Debye-Scherrer arc spreading, X-ray diffraction peak broadening, radiation
damage erasure, and electron spin resonance (ESR) Mn^{++} zero-crystal-field
splitting effects are all observed to vary <u>consistently</u> with depth within the
XC-1 core section. An additional, and very fortunate property of all the above
mentioned effects is their first-order <u>independence</u> of the relative abundance of
the carbonate polymorphs, aragonite and calcite, found in these rocks. Analogous
variations are observed in experimentally shocked specimens of both single-
crystal calcite and Eniwetok material sampled from areas unaffected by the Cactus
event. Comparing data from <u>in-situ</u> and laboratory recovered carbonates has
enabled us to place upper and lower limits on the stresses experienced at various
levels in the XC-1 core.

In addition to the already mentioned refinement of shock-effect detection
methods, further recovery experiments should allow us to more narrowly limit
shock pressures. Also, physical models providing a theoretical basis for the
processes which take place upon shock processing fine-grained carbonates are
presently under development. This understanding would be of considerable value
in predicting the response of shocked carbonate materials occurring in other

3

geologies. In the case of the electron spin resonance method, the work on the Cactus core material is, in fact, a pioneering effort in this area of research. It is likely that the results of this research program can be applied to other explosively shocked and meteorite impacted rocks.

RESEARCH SUMMARY
Angular Strain Analysis

A systematic increase in angular strain with pressure, analagous to that measured in laboratory shocked specimens, is displayed by calcite crystals isolated from XC-1 core material. (see Table 1.) Experimental single crystal calcite data provide a preliminary calibration curve relating observed strain to a documented shock pressure (Figure 1). In addition to such an empirical correlation, a theoretical model based on compressional data of Ahrens and Gregson (1964) has been applied to the material. Knowing the pressure-volume behavior of a mineral, shock pressure may be explicitly related to angular strain, θ_m, by the following relation

$$\theta_m = \tan^{-1}\left[\sqrt{\frac{V_o}{V}}\right] - \tan^{-1}\left[\sqrt{\frac{V}{V_o}}\right] \tag{1}$$

V_o and V represent initial and compressed volumes, respectively. Equation (1) is applicable in the region of deformational behavior at pressures not exceeding those of a shock-induced phase change which, in calcite, occurs at ∿16-17 kbar (Ahrens and Gregson, 1964). According to this model, it is inferred that calcite from a depth of 41.8' to 43' has been exposed to peak pressures of approximately 10 ± 5 kbars. Calcite from depths of ∿90' indicates strains corresponding to less than ∿5 kbars.

As first observed by R. Couch, aragonite displays a more consistent variation of Debye-Scherrer pattern angular broadening with depth, i.e., shock deformation, than does calcite. However, an extensive series of shock recovery experiments on single crystal aragonite, followed by Debye-Scherrer investigations of these samples, will be required before an observed-angular-strain to impact-stress relationship can be quantified. We propose to do just this in the future. A comparison of calculated stress levels from angular strain in both aragonite and calcite would serve to verify and more narrowly limit the shock

4

pressure inferred for same depth in the core. Toward this end, preliminary equation of state data for aragonite has been obtained during the present project.

TABLE 1

Ni-K$_\alpha$ Debye-Scherrer Reflection Strain Angles[a]

A. CIT Shocked Calcite[b], Single Crystal (101)

Diffraction Line Arc (°), Rhombic Notation

Shock Pressure (kbar)	(102)	(100)	(113)	(202)	(204)	(208)
0.0[c]	0.00 ±.05	0.00 ±0.04	0.00 ±0.10	0.00 ±0.13	0.00 ±0.093	0.00 ±0.11
7	0.25 ±0.21	0.46 ±0.30	0.26 ±0.19	0.68 ±0.20	0.17 ±0.17	0.23 ±0.25
36	1.23 ±0.63	2.23 ±1.37	1.76 ±1.06	1.81 ±0.89	1.27 ±1.09	1.55 ±0.90

B. Calcite Crystals from Cactus, XC-1 Core Hole

Diffraction Line Arc (°), Rhombic Notation

Core Interval (feet)	(102)	(100)	(113)	(202)	(204)	(200)
41.4-48	0.38* ±0.18	1.03 ±0.97	0.20 ±0.27	0.46 ±0.47	0.29 ±0.20	0.17 ±0.18
83-87	0.30* ±0.11	0.19 ±0.18	0.38 ±1.22	0.22* ±0.09	0.24* ±0.16	0.26* ±0.03
87-91	0.25* ±0.06	0.31 ±0.43	0.02 ±0.15	0.17 ±0.16	0.16 ±0.15	0.15 ±0.15

---

a) X-ray diffraction patterns taken by R. Couch.
b) Samples supplied by F. Hörz.
c) Sample, AFWL Standard calcite #6, unshocked sample gave 0.04 to 0.11°, natural beam width. The natural beam width has been subtracted from data for each diffraction peak.
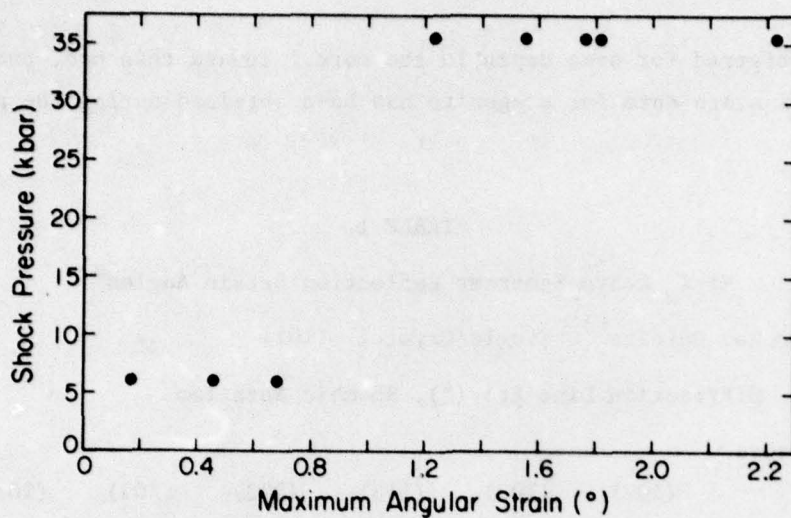* Lowest uncertainty, angular strain data.

5

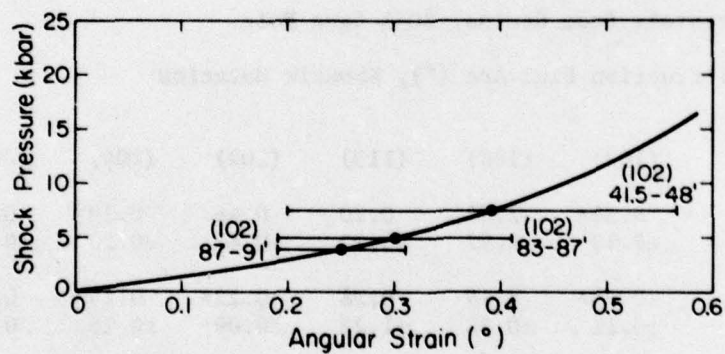Figure 1. Maximum angular strain vs. pressure in shock
recovered calcite.

Figure 2. Preliminary shock pressure vs. angular strain
based on Equation (1). Data plotted are for
(102) calcite reflection.

Particle Size Analysis

Powder X-ray diffraction spectra of XC-1 core material display a systematic decrease in broadening of both calcite and aragonite peaks, measured at half their maximum intensity, with increasing depth of sample. Tracings were obtained with a standard 45 Kv-Cu X-ray goniometer; unstrained, biogenic calcite was used as a reference standard. Diffraction peak broadening is known to be related to the mean dimension, D, of the crystallites composing the powder according to the following equation from Klug and Alexander, p. 491:

$$D = \frac{K\lambda}{\beta\cos\theta} \tag{2}$$

K is a constant related to the crystallite shape, λ is the wave length of the X-rays, θ the Bragg reflection angle for the (102) calcite peak, and β the half-width of that peak at half-maximum intensity.

The variation in crystallite size with depth in the XC-1 Cactus core is plotted in Figure 3. Although data points from intermediate to lower core samples show considerable scatter, those from the uppermost levels are significantly displaced toward the fine end of the granulation scale. Comparison with recovery data indicates that the shallow XC-1 material was exposed to pressures in excess of 2 kbars. Successful recoveries of saturated core material shocked to $\sim$20 kbars have been achieved, but X-ray diffraction data on these samples is not yet available.
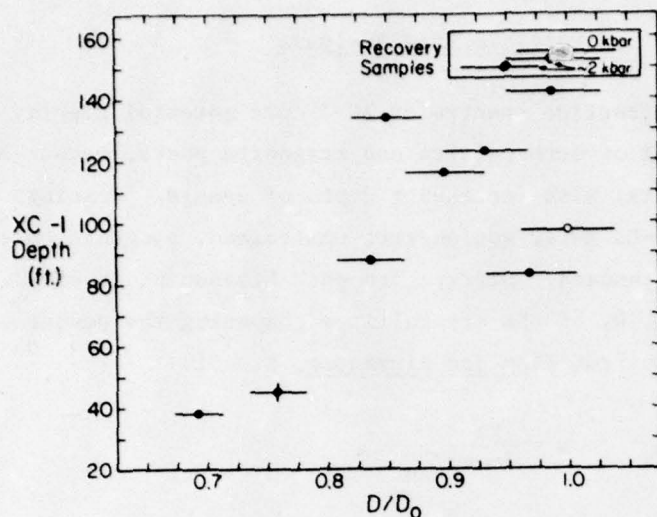
Figure 3. Variation of mean crystallite dimension, D, relative to that of unstrained biogenic calcite, D_o, as inferred from calcite (102) peak broadening. Preliminary data for grain sizes in two shock-recovered water-saturated cores (10' depth, XRU-3) and a control sample (0.0 kbar) are also indicated.

Shock-Induced Erasure of Radiation Damage Centers

The electron spin resonance peak attributed to intracrystalline radiation damage displays a unique pattern in spectra of laboratory and Cactus explosion shocked specimens. Natural U^{238}, K^{40}, and cosmic ray influences are believed to produce vacancies in the $CO_3^=$ sites of both aragonite and calcite; the observed spectral peak is presumably due to the resonance of free electrons occupying these vacancies. Comparison of unshocked and laboratory shocked (2→17 kbars) carbonates indicates that the intensity of this feature consistently decays with the application of increasing stresses. It is hypothesized that shocked induced annealing provides the erasure mechanism. Figure 4 depicts the variation in radiation damage peak with depth in the XC-1 Cactus core. As seen in this diagram, heating the specimens to 430°C somewhat decreases the amplitude of this feature. However, the depth vs. intensity pattern remains unaltered and shock rather than thermal erasure is concluded to be the dominant mechanism. A detailed series of chemical analyses would be required to accurately calibrate this effect in terms of applied shock stress. Of interest is the high level of

8

ESR radiation damage observed in the 36.5' (approximately the fall-back breccia-in-situ rock interface level). This radiation damage is unaffected by heating to 430°C and is considerably greater than seen in any of the other core material. This material may have experienced high fluxes of gammas and low-energy neutrons. On a simplistic level, the total radiation dose of this material may be calibratable. That this is so, is suggested by a preliminary experiment in which a Co^{60} source was used to irradiate Iceland spar with a dose of 1.2×10^6 rads (Figure 5G) and annealing at 600°C for 20 min., Figure 5H.

We thus, tentatively, interpret the amplitude of the relative damage ESR spectrum versus depth (Figure 4) as resulting from two competing effects as follows: the non-thermal or non-shock eraseable peak in the uppermost core appears to be radiatively induced by the device...this effect decays to a negligible value at a depth of between 46' to 89' below which the shock wave appears to have attenuated the natural radiative damage spectral resonance peak, the latter effect decreasing with depth.
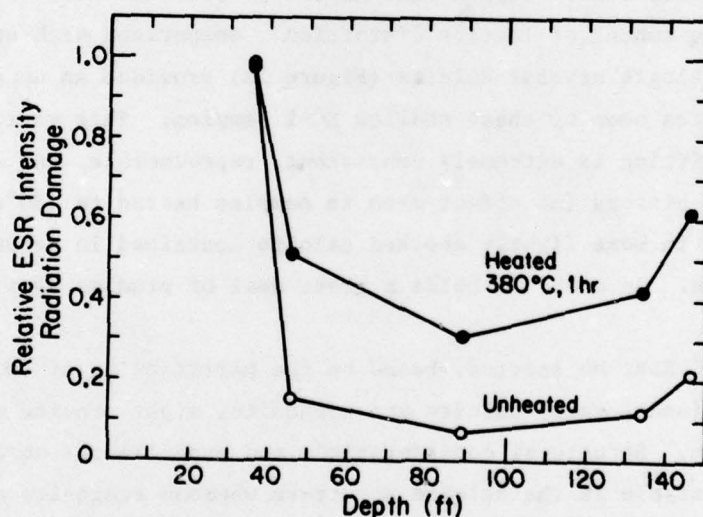

Figure 4. Relative intensity of radiation-damage ESR peak at ∿3300 Gauss at 9.1 GHz versus depth for XC-1 core, from Cactus crater unheated and heated to 430°C for one hour. Two effects are superimposed. At shallow depth, the non-erasable device-induced radiation damage dominates, whereas between ∿90 to ∿145 ft. the natural radiation damage is progressively less-erased as the result of the decaying shock wave.

9

Lattice Distortion Effects-Evidence From Mn^{++}

The sensitivity of the ESR method to paramagnetic elements allows for the
detection of both the presence and structural positioning of Mn^{++}, a common
trace constituent of carbonates, substituting for Ca^{++} in the crystal lattice.
In an undistorted octahedral environment (6 oxygen anions surrounding a Mn^{++}
ion) provided by the calcite structure, the $3d^5$ electrons of Mn^{++} assume an
energetically favorable configuration known in crystal field theory as "zero-
field" splitting. This "energy distribution" appears in the ESR Mn^{++} spectra
as a distinctive doublet feature (9.1 GHz resonance at $\sim$3540 Gauss) corresponding
to the transition $I = 5/2$, $S = +1/2 \rightarrow S = -1/2$. A severe change in the ligand
field and/or disturbance of host lattice structure appears to introduce a five-
fold electron spin degeneracy which is reflected in the ESR spectra ($\sim$3540 Gauss)
as a single peak. A consistent increase in the amount of splitting, and hence,
decreasing shock deformation with depth is observed for XC-1 core samples
(Figures 5 & 6). In particular, samples from depths of 36.5 and 41.4$\rightarrow$48.1 feet
indicate a considerable amount of lattice distortion. Comparison with spectra
of laboratory shocked single crystal calcite (Figure 5A) provides an upper limit
of 55 kbars for pressures seen by these shallow XC-1 samples. This variation
in Mn^{++} zero-field splitting is extremely consistent, reproducible, and apparently
independent of thermal history (no effect seen in samples heated to 430°C). It
has also been observed in some lightly shocked calcite contained in several
carbonaceous meteorites. As such, it holds a great deal of promise as a stress
level indicator.

Another feature of ESR, Mn spectra, based on the partitioning of two Mn oxi-
dation states between (undeformed) calcite and aragonite, might provide a means
of pressure calibration. Structural considerations and experimental observations
indicate that Mn^{++} is stable in the calcite structure whereas aragonite accommo-
dates Mn^{+++} (Low & Zeira, 1972). However, shocking the aragonite possibly
affects its crystal lattice so that it can no longer provide a stable configura-
tion for Mn^{+++} (Gibbons, Ahrens & Rossman, 1974). Under such deforming conditions
and in the presence of a reducing ionic species (abundant in an aqueous environ-
ment) Mn^{+++} is reduced to Mn^{++}. Since the partitioning of these two states is
effectively complete and the temperature contribution to the reducing transition
apparently minimal, only Mn^{++} detected in aragonite might be explained as a shock
pressure effect. Such an effect is very tentatively indicated by analyses of

10

core material experimentally shocked in the 2→17 kbar range. However, its variation is not consistent and numerical shock pressures cannot at this time be inferred from the data. The consistency may be observed by widely varying Mn content (unknown) and aragonite-calcite ratios (aragonite content varies erratically from 0→94% in the XC-1 core); further chemical analyses will be required before the validity of this method can be established.
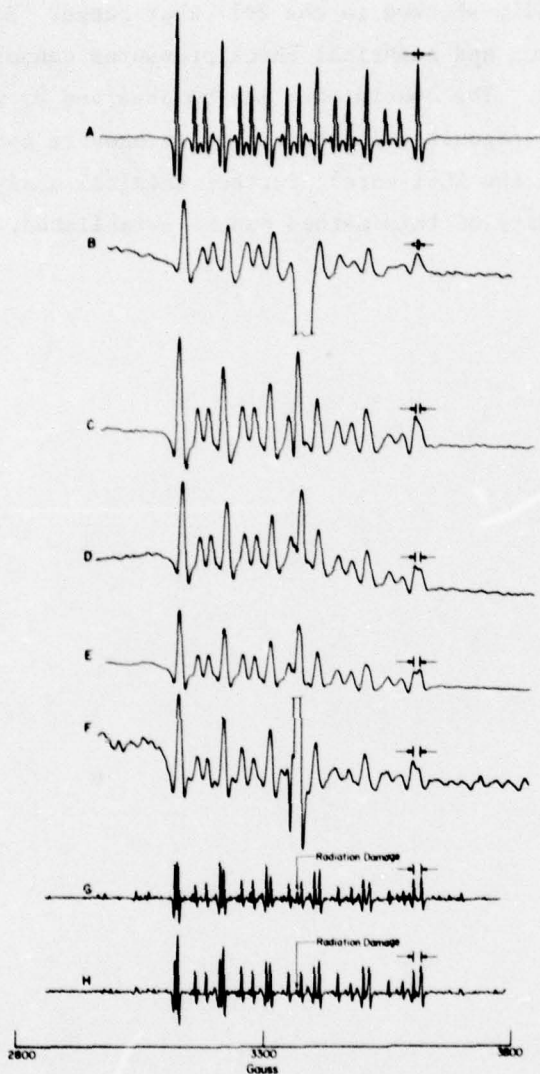
Figure 5.   ESR spectra taken at 9.1 GHz.   Splitting of ∿3540 Gauss
peak is indicated above the right hand side of each spectrum.
A = Shot #117, pure calcite shocked to 55 kbar.   Note complete
absence of 3540 Gauss split peak.   B = spectra of most intensely
shocked Cactus sample from a depth of 36.5 ft., XC-1.   Note
absence of 3540 Gauss split peak.   C = 41.4-48.1 ft., XC-1.
D = 87-91 ft., XC-1.   E = 133-135 ft., XC-1.   F = 146 ft., XC-1.
G = pure calcite unshocked; notice very wide doublet in spectra
at 3540 Gauss and radiation-induced damage peak ∿3300 Gauss
produced by exposure to 1.2 x 10^6 rads of Co^{60} radiation.
H = same sample as in G, except radiation-induced damage peak
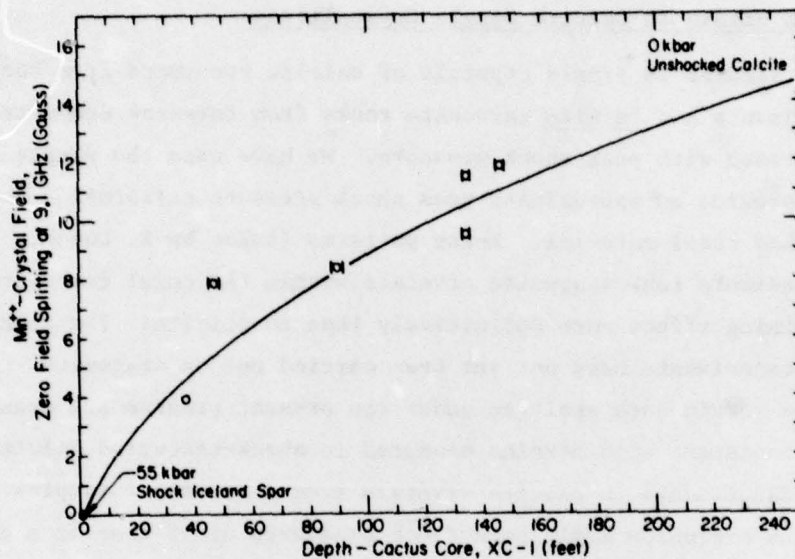partially annealed by application 600°C for 20 min.

12

Figure 6. Magnitude of "zero-field" splitting of ∿3540
Gauss peak versus depth. Magnitude of splitting
of 55 kbar shocked calcite and unshocked calcite
shown for conceptual purposes only.

CONCLUSION

It appears possible, by examining non-elastic permanent deformations of
very small crystallites of carbonate minerals, such as occur in the Eniwetok
cores, to relate these deformations via possibly four different shock effects,
to peak shock pressure and appropriate equations of state. The techniques which
appear applicable, and in some cases, have already tentatively been applied to
determining peak shock pressures for aliquots of core taken directly beneath
the Cactus explosion (Eniwetok) are:

(1) <u>Peak Broadening in X-Ray Powder Diffractometer Spectra</u>.

We have observed a systematic decrease of the effective size of the
average diffracting crystallites of calcite and aragonite for successively more
intensely shocked <u>in-situ</u> coral material. Samples recovered from ∿2 kbar stress
levels, indicate a slight decrease in crystallite size similar to that observed
in the rock at depths of ∿50 m at the Cactus site. Detailed analysis of aliquots
of initially unshocked coral, shocked in the laboratory has not yet been carried
out.

13

(2) <u>Angular Strain in Calcite Single Crystallites</u>.

The angular strains in single crystals of calcite recovered from both laboratory experiments and <u>in-situ</u> carbonate rocks from Eniwetok demonstrate a systematic increase with peak shock pressure. We have used the single crystal data to provide an approximate peak shock pressure calibration for the <u>in-situ</u> shocked coral material. X-ray patterns (taken by R. Couch, McClellan AFB) indicate that aragonite crystals within the coral demonstrate the angular straining effect more definitively than in calcite. The appropriate calibration experiments have not yet been carried out on aragonite.

Although the strain data analyzed under the present program are scanty, they are not inconsistent with strains measured in shock-recovered calcite. Angular strain measurements in calcite crystals from a series of samples from beneath the Cactus explosion imply peak shock pressures of ∿8 kbar at a depth of ∿15 m decaying to ∿3 kbar at a depth of ∿30 m. These values are, at present, tentative. We expect upon examination of shock deformation in aragonite to obtain a better grasp on the shock-wave amplitudes.

(3) <u>Shock-Induced Erasure of Defect Spectra in Calcite</u>.

Electron-spin resonance spectra for a series of aliquotes of shocked carbonate material, both shocked in the laboratory and by the Cactus explosion, demonstrate the major feature observed is the resonance of an electron in a $CO_3^=$ vacancy. This feature which is presumed to arise from the natural radiogenic sources is apparently very sensitive to the stress history of calcite. A systematic decrease in amplitude of this resonance, which occurs at ∿3300 Gauss and 9.1 GHz, is observed to occur for material shocked in the laboratory over the range 2 to 17 kbar. A similar change in spectra is observed in samples explosively shocked, <u>in-situ</u>. A detailed series of measurements to "calibrate" this effect in terms of strain, and ultimately, shock stress, has not yet been carried out.

(4) <u>Effect of Shock on Zero-Field Splitting of Mn^{++} in Calcite</u>.

Recently we discovered a systematic loss of fine structure in electron spin resonance spectrum arising from Mn^{++}, substituting for Ca^{++} in calcite for samples exposed to increasing amplitude shock waves in the 2 to 38 kbar range. A similar variation with depth, and hence, effectively shock pressure, is observed in shocked coral from Eniwetok and also in some lightly shocked calcite in several meteorites.

14

REFERENCES

Ahrens, T. J., and V. G. Gregson, 1964. Shock compression of crustal rocks: data for quartz, calcite and plagioclase rocks, J. Geophys. Res., 69, 4839-4874.

Ahrens, T. J., and R. K. Linde, 1968. Response of brittle solids to shock compression, in Behavior of Dense Media Under High Dynamic Pressures, Proc. Symposium High Dynamic Pressure, Paris, 1967, Gordon and Breach, New York, pp. 325-336.

Gibbons, R. V., T. J. Ahrens and G. R. Rossman, 1974. A spectroscopic interpretation of the shock-produced color change in Rhodonite ($MnSiO_3$): The shock-induced reduction of MnIII to MnII, American Mineralogist, 59, 177-182.

Klug, H. P., and L. E. Alexander, 1954. X-ray Diffraction Procedures, John Wiley, New York.

Low, W., and S. Zeira, 1972. ESR spectra of Mn^{2+} in heat-treated aragonite, American Mineralogist, 57, 1115-1124.

DISTRIBUTION LIST

DEPARTMENT OF THE AIR FORCE

Air Force Geophysics Laboratory
    ATTN: LWW, K. Thompson

Air Force Institute of Technology, Air University
    ATTN: Library

Air Force Systems Command
    ATTN: DLW

Air Force Weapons Laboratory
    ATTN: DE, M. Plamondon
    ATTN: SUL
    ATTN: DES, J. Shinn
    ATTN: DES, J. Thomas

Assistant Chief of Staff, Intelligence
Department of the Air Force
    ATTN: INT

Deputy Chief of Staff, Research, Development, & ACQ
Department of the Air Force
    ATTN: AFRDQSM

Foreign Technology Division, AFSC
Department of the Air Force
    ATTN: NIIS Library

Rome Air Development Center, AFSC
Department of the Air Force
    ATTN: Documents Library

Space & Missile Systems Organization
Department of the Air Force
    ATTN: MNN

Strategic Air Command
    ATTN: NRI-STINFO Library

DEPARTMENT OF ENERGY

Department of Energy
Albuquerque Operations Office
    ATTN: Doc. Con. for Technical Library

Department of Energy
Library Room G-042
    ATTN: Doc. Con. for Classified Library

Department of Energy
Nevada Operations Office
    ATTN: Doc. Con. for Technical Library

DEPARTMENT OF ENERGY CONTRACTORS

Lawrence Livermore Laboratory
    ATTN: Tech. Info. Dept. Library
    ATTN: L-96, L. Woodruff

Los Alamos Scientific Laboratory
    ATTN: Reports Library
    ATTN: R. Bridwell

Oak Ridge National Laboratory
Union Carbide Corporation, Nuclear Division
X-10 Lab Records Division
    ATTN: Technical Library
    ATTN: Civil Def. Res. Proj.

DEPARTMENT OF ENERGY CONTRACTORS (Continued)

Sandia Laboratories
    ATTN: L. Hill
    ATTN: 3141
    ATTN: S. Chabai

Sandia Laboratories, Livermore
    ATTN: Library & Security Class. Div.

OTHER GOVERNMENT

Central Intelligence Agency
    ATTN: J. Ingley

Department of the Interior
Bureau of Mines
    ATTN: Technical Library

DEPARTMENT OF DEFENSE CONTRACTORS

Aerospace Corporation
    ATTN: Technical Information Services

Agbabian Associates
    ATTN: M. Agbabian

Applied Theory, Inc.
 2 cy ATTN: J. Trulio

AVCO Research & Systems Group
    ATTN: Library A830

BDM Corporation
    ATTN: Corporate Library
    ATTN: T. Neighbors

Boeing Company
    ATTN: Aerospace Library

California Institute of Technology
    ATTN: T. Aherns
    ATTN: J. Vizgirda

California Research & Technology, Inc.
    ATTN: D. Orphal

California Research & Technology, Inc.
    ATTN: S. Shuster
    ATTN: Library
    ATTN: K. Kreyenhagen

Calspan Corporation
    ATTN: Library

Civil/Nuclear Systems Corporation
    ATTN: J. Bratton

University of Dayton
Industrial Security Super KL-505
    ATTN: H. Swift

University of Colorado Seminary
Denver Research Institute
    ATTN: Sec. Officer for J. Wisotski

EG&G Washington Analytical Services Center, Inc.
    ATTN: Library

18

Eric H. Wang, Civil Engineering Rsch. Fac.
    ATTN: N. Baum

Gard, Incorporated
    ATTN: G. Neidhardt

General Electric Company-TEMPO
Center for Advanced Studies
    ATTN: DASIAC

IIT Research Institute
    ATTN: Documents Library
    ATTN: M. Johnson
    ATTN: R. Welch

University of Illinois, Consulting Services
    ATTN: N. Newmark

Institute for Defense Analyses
    ATTN: Classified Library

Kaman AviDyne, Division of Kaman Sciences Corp.
    ATTN: E. Criscione
    ATTN: Library
    ATTN: N. Hobbs

Kaman Sciences Corporation
    ATTN: Library

Lockheed Missiles & Space Company, Inc.
    ATTN: T. Geers
    ATTN: Technical Information Center

McDonnell Douglas Corporation
    ATTN: R. Halprin

Merritt CASES, Inc.
    ATTN: Library
    ATTN: J. Merritt

Physics International Company
    ATTN: F. Sauer
    ATTN: L. Behrmann
    ATTN: Technical Library
    ATTN: E. Moore
    ATTN: J. Thomsen

R&D Associates
    ATTN: C. MacDonald
    ATTN: J. Lewis
    ATTN: R. Port
    ATTN: Technical Information Center
    ATTN: A. Latter

R&D Associates
    ATTN: H. Cooper

SRI International
    ATTN: B. Gasten
    ATTN: G. Abrahamson
    ATTN: D. Keough
    ATTN: Y. Gupta

Systems, Science & Software, Incorporated
    ATTN: D. Grine
    ATTN: Library
    ATTN: T. Riney
    ATTN: T. Cherry

Systems, Science & Software, Inc.
    ATTN: J. Murphy

Terra Tek, Incorporated
    ATTN: S. Green
    ATTN: Library
    ATTN: A. Abou-Sayed

Tetra Tech, Incorporated
    ATTN: Library

TRW Defense & Space Systems Group
    ATTN: Technical Information Center
2 cy ATTN: P. Dai
    ATTN: P. Bhutta

TRW Defense & Space Systems Group
San Bernardino Operations
    ATTN: E. Wong

Vela Seismological Center
    ATTN: G. Ulrich

Weidlinger Assoc., Consulting Engineers
    ATTN: M. Baron
    ATTN: I. Sandler

Weidlinger Assoc., Consulting Engineers
    ATTN: J. Isenberg

Science Applications, Incorporated
    ATTN: Technical Library

Science Applications, Incorporated
    ATTN: D. Maxwell
    ATTN: D. Bernstein

Southwest Research Institute
    ATTN: W. Baker
    ATTN: A. Wenzel